Meccanica (2006) 41:79–99
DOI 10.1007/s11012-005-8866-9

An Interface Crack for a Functionally Graded Strip Sandwiched Between Two Homogeneous Layers of Finite Thickness

ZHEN-GONG ZHOU* and BIAO WANG
Center for Composite Materials, Harbin Institute of Technology, P.O.Box 1247, Harbin 150001, P.R.China

(Received: 31 January 2003; accepted in revised form: 21 April 2005)

Abstract. In this paper, the behavior of an interface crack for a functionally graded strip sandwiched between two homogeneous layers of finite thickness subjected to an uniform tension is resolved using a somewhat different approach, named the Schmidt method. The Fourier transform technique is applied and a mixed boundary value problem is reduced to two pairs of dual integral equations in which the unknown variables are the jumps of the displacements across the crack surface. To solve the dual integral equations, the jumps of the displacements across the crack surfaces are expanded in a series of Jacobi polynomials. This process is quite different from those adopted in previous works. Numerical examples are provided to show the effects of the crack length, the thickness of the material layer and the materials constants upon the stress intensity factor of the cracks. It can be obtained that the results of the present paper are the same as ones of the same problem that was solved by the singular integral equation method. As a special case, when the material properties are not continuous through the crack line, an approximate solution of the interface crack problem is also given under the assumption that the effect of the crack surface interference very near the crack tips is negligible. Contrary to the previous solution of the interface crack, it is found that the stress singularities of the present interface crack solution are the same as ones of the ordinary crack in homogenous materials.

Key words: Interface crack, Functionally graded materials, Schmidt method, Dual integral equations.

1. Introduction

The analysis of functionally graded materials has become a subject of increasing importance motivated by a number of potential benefits achievable from the use of such novel materials in a wide range of modern technological practices. The major advantages of graded materials, especially in elevated temperature environments, stem from the tailoring capability to produce a gradual variation of its thermomechanical properties in the spatial domain [1]. In particular, the use of a graded material as an interlayer between bonded media, is one of the highly effective and promising applications in eliminating various shortcoming resulting from stepwise property mismatch inherent in piecewise homogeneous composite media [2–4].

From the fracture mechanics viewpoint, the presence of a graded interlayer would play an important role in determining the crack driving forces and fracture resistance

*Author for correspondence: e-mail: zhouzhg@hit.edu.cn

parameters. In an attempt to address the issues pertaining to the fracture analysis of bonded media with such transitional interfacial properties, a series of solutions to certain crack problems was obtained by Erdogan and his associates [5–7]. Among them there are the solutions for a crack in the non-homogeneous interlayer bounded by dissimilar homogeneous media [5]; and for a crack at the interface between homogeneous and non-homogeneous materials [6, 7]. Similar problems of delamination or an interface crack between a functionally graded coating and a substrate were considered in [8–10]. The dynamic crack problem for non-homogeneous composite materials was considered in [11] but the authors considered the FGM layer as a multi-layered homogeneous medium. The crack problem in FGM layers under thermal stresses was studied by Erdogan and Wu [12]. They considered an unconstrained elastic layer under statically self-equilibrating thermal or residual stresses and the layer contained an embedded or surface crack perpendicular to its boundaries.

In this paper, the same problem that was treated by Shbeeb and Binienda [10] is reworked using a somewhat different approach, named the Schmidt method [13–16]. The Fourier transform technique is applied and a mixed boundary value problem is reduced to two pairs of dual integral equations in which the unknown variables are the jumps of the displacements across the crack surface. To solve the dual integral equations, the jumps of the displacements across crack surfaces are expanded in a series of Jacobi polynomials. This process is quite different from those adopted in the references [1–12] as mentioned above. In the previous works [1–12], the unknown variables of dual integral equations are the dislocation density functions. This is the major difference. The numerical results are the same as in [10] when the material properties are continuous through the crack line. It is also proved that the Schmidt method is performed satisfactorily. On the other hand, as discussed in [17], an exact solution of the interface crack problem had been given in [18] in spite of the incomprehensibility in fracture mechanics. However, from an engineering viewpoint, it is more desirable to seek a solution that is physically acceptable. Hence, the solving process of the present paper is expanded to solve the special case problem when the material properties are not continuous through the crack line. In this case, an approximate solution of the interface crack problem is given under the assumption that the effect of the crack surface interference very near the crack tips is negligible as discussed in [19–21]. For this special case (From practical view points, researchers in the field of functionally graded materials will not pay their attention in this case), it is found that the stress singularities of the present interface crack solution are the same as ones of the ordinary crack in homogeneous materials, while much problems have to be considered when the material properties are not continuous through the crack line.

2. Formulation of the Problem

The geometry of the problem is shown in Figure 1. Both the coating and the substrate, which are perfectly bonded to the FGM layer, are isotropic and homogeneous, and have h_1 and h_3 as their respective thickness. The FGM layer thickness is h_2, and is denoted as material 2. Crack problems in the non-homogeneous materials do not appear to be analytically tractable for arbitrary variations of material properties. Usually, one tries to generate the forms of non- homogeneities for which the problem

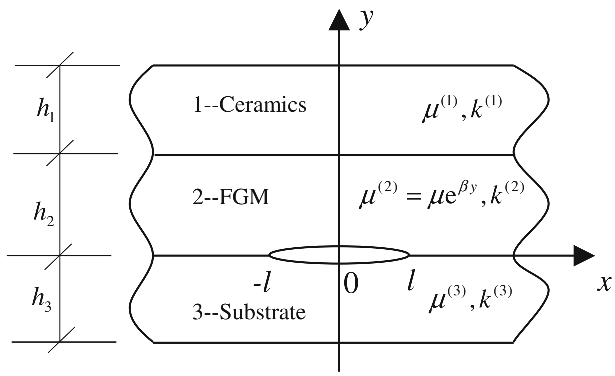

Figure 1. Geometry of the interface crack for a functionally graded layer sandwiched between two homogeneous layers.

becomes tractable. Similar to the treatment of the crack problem for isotropic non-homogeneous materials in [5,6], we assume the shear modulus of the FGM layer is assumed to be as follows

$$\mu^{(2)} = \mu e^{\beta y}, \tag{1}$$

where β is a constant. If $\mu = \mu^{(3)}$ and $\beta = \frac{1}{h_2} ln(\mu^{(1)}/\mu^{(3)})$, the problem in this paper will return to the same problem as discussed in [10].

The constitutive relations for the non-homogeneous material are written as

$$\sigma_x^{(j)}(x, y) = \frac{\mu^{(j)} e^{\beta y}}{k^{(j)} - 1}\left[(1 + k^{(j)})\frac{\partial u^{(j)}}{\partial x} + (3 - k^{(j)})\frac{\partial v^{(j)}}{\partial y}\right], \quad (j = 1, 2, 3), \tag{2}$$

$$\sigma_y^{(j)}(x, y) = \frac{\mu^{(j)} e^{\beta y}}{k^{(j)} - 1}\left[(1 + k^{(j)})\frac{\partial v^{(j)}}{\partial y} + (3 - k^{(j)})\frac{\partial u^{(j)}}{\partial x}\right], \quad (j = 1, 2, 3), \tag{3}$$

$$\tau_{xy}^{(j)}(x, y) = \mu^{(j)} e^{\beta y}\left[\frac{\partial u^{(j)}}{\partial y} + \frac{\partial v^{(j)}}{\partial x}\right], \quad (j = 1, 2, 3), \tag{4}$$

where $u^{(j)}(x, y)$and $v^{(j)}(x, y)$represent (The superscript $j = 1, 2, 3$ corresponds to the coating layer, the FGM layer and the substrate layer, respectively.) the displacement components in the x- and y-directions, respectively. $\sigma_x^{(j)}, \sigma_y^{(j)}$ and $\tau_{xy}^{(j)}$ $(j = 1, 2, 3)$ represent the Cartesian components of stress. $\mu^{(j)}$ $(j = 1, 2, 3)$ is the shear modulus. $k^{(j)} = 3 - 4\eta^{(j)}$ $(j = 1, 2, 3)$ for plane strain, $k^{(j)} = (3 - \eta^{(j)})/(1 + \eta^{(j)})$ $(j = 1, 2, 3)$ for the plane stress. $\eta^{(j)}$ $(j = 1, 2, 3)$ is the Poisson's ratio. The Poisson's ratio for the FGM layer, $\eta^{(2)}$, is taken to be a constant; owing to the fact that its variation within a practical range has an insignificant influence on the stress fields near the crack tips [5–7]. We assume that $\beta \neq 0$ for the graded interlayer and $\beta = 0$ for the coating layer and the substrate layer. In this paper, we just consider the plane strain problem.

In the absence of body forces, the elastic behavior of the medium with the variable shear modulus in equation (1) is governed by the following equations

$$(1 + k^{(j)})\frac{\partial^2 u^{(j)}}{\partial x^2} + (k^{(j)} - 1)\frac{\partial^2 u^{(j)}}{\partial y^2} + 2\frac{\partial^2 v^{(j)}}{\partial x \partial y} + (k^{(j)} - 1)\beta\left(\frac{\partial u^{(j)}}{\partial y} + \frac{\partial v^{(j)}}{\partial x}\right) = 0,$$
$$(j = 1, 2, 3), \tag{5}$$

$$(1+k^{(j)})\frac{\partial^2 v^{(j)}}{\partial y^2}+(k^{(j)}-1)\frac{\partial^2 v^{(j)}}{\partial x^2}+2\frac{\partial^2 u^{(j)}}{\partial x\partial y}+\beta\left[(1+k^{(j)})\frac{\partial v^{(j)}}{\partial y}+(3-k^{(j)})\frac{\partial u^{(j)}}{\partial x}\right]=0,$$
$$(j=1,2,3). \tag{6}$$

3. Solution

Because of the symmetry, it suffices to consider the problem for $x \geqslant 0, |y| < \infty$. The system of above governing equations is solved, using the Fourier integral transform technique to obtain the general expressions for the displacement components as

$$\begin{cases} u^{(1)} = \dfrac{2}{\pi}\displaystyle\int_0^\infty 2s^2\{[-A_1(s)+(1-sy)A_2(s)]\mathrm{e}^{-sy}+[A_3(s)+(1+sy)A_4(s)]\mathrm{e}^{sy}\}\sin(sx)\mathrm{d}s \\ v^{(1)} = \dfrac{2}{\pi}\displaystyle\int_0^\infty 2s^2\{[-A_1(s)-(k^{(1)}-1+sy)A_2(s)]\mathrm{e}^{-sy} \\ \qquad +[-A_3(s)+(k^{(1)}-1-sy)A_4(s)]\mathrm{e}^{sy}\}\cos(sx)\mathrm{d}s \end{cases} \tag{7}$$

$$\begin{cases} u^{(2)} = \dfrac{2}{\pi}\displaystyle\int_0^\infty \sum_{i=1}^4 B_i(s)\mathrm{e}^{-\lambda_i y}\sin(sx)\mathrm{d}s, \\ v^{(2)} = \dfrac{2}{\pi}\displaystyle\int_0^\infty \sum_{i=1}^4 m_i(s)B_i(s)\mathrm{e}^{-\lambda_i y}\cos(sx)\mathrm{d}s, \end{cases} \tag{8}$$

$$\begin{cases} u^{(3)} = \dfrac{2}{\pi}\displaystyle\int_0^\infty 2s^2\{[-C_1(s)+(1-sy)C_2(s)]\mathrm{e}^{-sy}+[C_3(s)+(1+sy)C_4(s)]\mathrm{e}^{sy}\}\sin(sx)\mathrm{d}s, \\ v^{(3)} = \dfrac{2}{\pi}\displaystyle\int_0^\infty 2s^2\{[-C_1(s)-(k^{(3)}-1+sy)C_2(s)]\mathrm{e}^{-sy}+[-C_3(s)+(k^{(3)}-1-sy) \\ \qquad C_4(s)]\mathrm{e}^{sy}\}\cos(sx)\mathrm{d}s \end{cases} \tag{9}$$

and from equations (2)–(4), the stress components are obtained as

$$\sigma_y^{(1)} = \frac{2\mu^{(1)}}{\pi}\int_0^\infty 2s^3\{[2A_1(s)+(k^{(1)}-1+2sy)A_2(s)]\mathrm{e}^{-sy} \\ +[-2A_3(s)-(1-k^{(1)}+2sy)A_4(s)]\mathrm{e}^{sy}\}\cos(sx)\mathrm{d}x, \tag{10}$$

$$\tau_{xy}^{(1)} = \frac{2\mu^{(1)}}{\pi}\int_0^\infty 2s^3\{[2A_1(s)+(-3+k^{(1)}+2sy)A_2(s)]\mathrm{e}^{-sy} \\ +[2A_3(s)+(3-k^{(1)}+2sy]\mathrm{e}^{sy}\}\sin(sx)\mathrm{d}s, \tag{11}$$

$$\sigma_y^{(2)} = \frac{2\mu\mathrm{e}^{\beta y}}{\pi(k^{(2)}-1)}\int_0^\infty \sum_{i=1}^4[-(k^{(2)}+1)m_i(s)\lambda_i+s(3-k^{(2)})]B_i(s)\mathrm{e}^{-\lambda_i y}\cos(sx)\mathrm{d}s,$$
$$\tag{12}$$
$$\tau_{xy}^{(2)} = \frac{2\mu\mathrm{e}^{\beta y}}{\pi}\int_0^\infty \sum_{i=1}^4[-\lambda_i-m_i(s)s]B_i(s)\mathrm{e}^{-\lambda_i y}\sin(sx)\mathrm{d}s,$$

$$\sigma_y^{(3)} = \frac{2\mu^{(3)}}{\pi} \int_0^\infty 2s^3\{[2C_1(s) + (k^{(3)} - 1 + 2sy)C_2(s)]\mathrm{e}^{-sy} \\ + [-2C_3(s) - (1 - k^{(3)} + 2sy)C_4(s)]\mathrm{e}^{sy}\}\cos(sx)\mathrm{d}x \tag{13}$$

$$\tau_{xy}^{(3)} = \frac{2\mu^{(3)}}{\pi} \int_0^\infty 2s^3\{[2C_1(s) + (-3 + k^{(3)} + 2sy)C_2(s)]\mathrm{e}^{-sy} \\ + [2C_3(s) + (3 - k^{(3)} + 2sy]\mathrm{e}^{sy}\}\sin(sx)\mathrm{d}s \tag{14}$$

where s is the transform variable, A_i, B_i and C_i, $i = 1, 2, 3, 4$, are arbitrary unknowns, $\lambda_i(s)$, $i = 1, 2, 3, 4$, are the roots of the characteristic equation

$$\lambda^4 - 2\lambda^3\beta + (\beta^2 - 2s^2)\lambda^2 + 2\beta s^2\lambda + s^4 + \frac{3 - k^{(2)}}{k^{(2)} + 1}\beta^2 s^2 = 0 \tag{15}$$

and $m_i(s)$ $i = 1, 2, 3, 4$, are expressed for each root $\lambda_i(s)$ as

$$m_i(s) = \frac{-(k^{(2)} + 1)s^2 + (k^{(2)} - 1)\lambda_i^2 - \beta(k^{(2)} - 1)\lambda_i}{-2s\lambda_i + s\beta(k^{(2)} - 1)}. \tag{16}$$

Equation (16) can be rewritten as the following form

$$(\lambda^2 - \lambda\beta - s^2)^2 + \frac{3 - k^{(2)}}{k^{(2)} + 1}\beta^2 s^2 = 0. \tag{17}$$

The roots may be obtained as

$$\lambda_1 = \frac{\beta + \sqrt{\beta^2 + 4\left(s^2 + i\beta s\sqrt{\frac{3 - k^{(2)}}{k^{(2)} + 1}}\right)}}{2}, \qquad \lambda_2 = \frac{\beta + \sqrt{\beta^2 + 4\left(s^2 - i\beta s\sqrt{\frac{3 - k^{(2)}}{k^{(2)} + 1}}\right)}}{2}, \tag{18}$$

$$\lambda_3 = \frac{\beta - \sqrt{\beta^2 + 4\left(s^2 + i\beta s\sqrt{\frac{3 - k^{(2)}}{k^{(2)} + 1}}\right)}}{2}, \qquad \lambda_4 = \frac{\beta - \sqrt{\beta^2 + 4\left(s^2 - i\beta s\sqrt{\frac{3 - k^{(2)}}{k^{(2)} + 1}}\right)}}{2}. \tag{19}$$

From equations (10) to (14), it can be seen that there are 12 unknown constants (in Fourier space they are functions of s), *i.e.*, A_i, B_i and C_i, $i = 1, 2, 3, 4$, which can be obtained from the following conditions:

$$\sigma_y^{(1)}(x, h_1 + h_2) = 0, \qquad \tau_{xy}^{(1)}(x, h_1 + h_2) = 0, \tag{20}$$

$$\sigma_y^{(1)}(x, h_2) = \sigma_y^{(2)}(x, h_2), \qquad \tau_{xy}^{(1)}(x, h_2) = \tau_{xy}^{(2)}(x, h_2), \tag{21}$$

$$u^{(1)}(x, h_2) = u^{(2)}(x, h_2), \qquad v^{(1)}(x, h_2) = v^{(2)}(x, h_2), \tag{22}$$

$$\sigma_y^{(3)}(x, -h_3) = 0, \qquad \tau_{xy}^{(3)}(x, -h_3) = 0, \tag{23}$$

$$\sigma_y^{(2)}(x, 0) = \sigma_y^{(3)}(x, 0) = -\sigma_0, \qquad \tau_{xy}^{(2)}(x, 0) = \tau_{xy}^{(3)}(x, 0) = 0, \quad |x| \leqslant l, \tag{24}$$

$$\sigma_y^{(2)}(x,0)=\sigma_y^{(3)}(x,0), \qquad \tau_{xy}^{(2)}(x,0)=\tau_{xy}^{(3)}(x,0), \qquad |x|>l, \tag{25}$$

$$u^{(2)}(x,0)=u^{(3)}(x,0), \qquad v^{(2)}(x,0)=v^{(3)}(x,0), \qquad |x|>l. \tag{26}$$

To solve the problem, the jumps of the displacements across the crack surfaces can be defined as follows:

$$f_1(x)=u^{(2)}(x,0)-u^{(3)}(x,0), \tag{27}$$

$$f_2(x)=v^{(2)}(x,0)-v^{(3)}(x,0), \tag{28}$$

where $f_1(x)$ is an odd function, $f_2(x)$ is an even function.

Applying the Fourier transform and the boundary conditions (20)–(26), it can be obtained

$$[X_1]\begin{bmatrix}A_1(s)\\A_2(s)\end{bmatrix}+[X_2]\begin{bmatrix}A_3(s)\\A_4(s)\end{bmatrix}=0, \tag{29}$$

$$[X_3]\begin{bmatrix}A_1(s)\\A_2(s)\end{bmatrix}+[X_4]\begin{bmatrix}A_3(s)\\A_4(s)\end{bmatrix}=[X_5]\begin{bmatrix}B_1(s)\\B_2(s)\end{bmatrix}+[X_6]\begin{bmatrix}B_3(s)\\B_4(s)\end{bmatrix}, \tag{30}$$

$$[X_7]\begin{bmatrix}A_1(s)\\A_2(s)\end{bmatrix}+[X_8]\begin{bmatrix}A_3(s)\\A_4(s)\end{bmatrix}=[X_9]\begin{bmatrix}B_1(s)\\B_2(s)\end{bmatrix}+[X_{10}]\begin{bmatrix}B_3(s)\\B_4(s)\end{bmatrix}, \tag{31}$$

$$[X_{11}]\begin{bmatrix}C_1(s)\\C_2(s)\end{bmatrix}+[X_{12}]\begin{bmatrix}C_3(s)\\C_4(s)\end{bmatrix}=0, \tag{32}$$

$$[X_{13}]\begin{bmatrix}C_1(s)\\C_2(s)\end{bmatrix}+[X_{14}]\begin{bmatrix}C_3(s)\\C_4(s)\end{bmatrix}=[X_{15}]\begin{bmatrix}B_1(s)\\B_2(s)\end{bmatrix}+[X_{16}]\begin{bmatrix}B_3(s)\\B_4(s)\end{bmatrix}, \tag{33}$$

$$[X_{17}]\begin{bmatrix}B_1(s)\\B_2(s)\end{bmatrix}+[X_{18}]\begin{bmatrix}B_3(s)\\B_4(s)\end{bmatrix}-[X_{19}]\begin{bmatrix}C_1(s)\\C_2(s)\end{bmatrix}-[X_{20}]\begin{bmatrix}C_3(s)\\C_4(s)\end{bmatrix}=\begin{bmatrix}\bar{f}_1(s)\\\bar{f}_2(s)\end{bmatrix}, \tag{34}$$

where the matrices $[X_i]$ $(i=1,2,3,\ldots,20)$ can be seen in Appendix A.

A superposed bar indicates the Fourier transform. If $f(x)$ is an even function, the Fourier transform is defined as follows:

$$\bar{f}(s)=\int_0^\infty f(x)\cos(sx)\mathrm{d}x, \qquad f(x)=\frac{2}{\pi}\int_0^\infty \bar{f}(s)\cos(sx)\mathrm{d}s. \tag{35}$$

If $f(x)$ is an odd function, the Fourier transform is defined as follows:

$$\bar{f}(s)=\int_0^\infty f(x)\sin(sx)\mathrm{d}x, \qquad f(x)=\frac{2}{\pi}\int_0^\infty \bar{f}(s)\sin(sx)\mathrm{d}s. \tag{36}$$

By solving 12 equations (29)–(34) with 12 unknown functions, substituting the solutions into equations. (12) and applying the boundary conditions, it can be obtained

$$\sigma_y^{(2)}(x,0)=\frac{2}{\pi}\int_0^\infty [d_1(s)\bar{f}_1(s)+d_2(s)\bar{f}_2(s)]\cos(sx)\mathrm{d}s=-\sigma_0,\quad 0\leqslant x\leqslant l, \tag{37}$$

$$\tau_{xy}^{(2)}(x,0)=\frac{2}{\pi}\int_0^\infty [d_3(s)\bar{f}_1(s)+d_4(s)\bar{f}_2(s)]\sin(sx)\mathrm{d}s=0,\quad 0\leqslant x\leqslant l, \tag{38}$$

$$\int_0^\infty \bar{f}_1(s)\sin(sx)\mathrm{d}s=0,\quad x>l, \tag{39}$$

$$\int_0^\infty \bar{f}_2(s)\cos(sx)\mathrm{d}s=0,\quad x>l, \tag{40}$$

where $d_1(s)$, $d_2(s)$, $d_3(s)$ and $d_4(s)$ are known functions (see Appendix A). To determine the unknown functions, $\bar{f}_1(s)$ and $\bar{f}_2(s)$, the above two pairs of dual integral equations (37)–(40) must be solved.

4. Solution of the Dual Integral Equations

To solve the problem, the jumps of the displacements across the crack surfaces can be represented by the following series: (When the material properties are not continuous through the crack line, as mentioned above, the problem is solved under the assumptions that the effect of the crack surface overlapping very near the crack tips is negligible. These assumptions had been used in [19–21]. It can be obtained that the jumps of the displacements across the crack surface are finite, differentiable and continuous functions. Only in this case, the jumps of the displacements across the crack surfaces can be represented by the following series:)

$$f_1(x)=\sum_{n=0}^\infty a_n P_{2n+1}^{(1/2,1/2)}\left(\frac{x}{l}\right)\left(1-\frac{x^2}{l^2}\right)^{\frac{1}{2}},\quad \text{for } 0\leqslant x\leqslant l, \tag{41}$$

$$f_1(x)=0, \text{for } x>l, \tag{42}$$

$$f_2(x)=\sum_{n=0}^\infty b_n P_{2n}^{(1/2,1/2)}\left(\frac{x}{l}\right)\left(1-\frac{x^2}{l^2}\right)^{\frac{1}{2}}\quad \text{for } 0\leqslant x\leqslant l, \tag{43}$$

$$f_2(x)=0\quad \text{for } x>l, \tag{44}$$

where a_n and b_n are unknown coefficients, $P_n^{(\frac{1}{2},\frac{1}{2})}(x)$ is a Jacobi polynomial [22]. The Fourier transforms of Eqs. (41)–(44) are [23]

$$\bar{f}_1(s)=\sum_{n=0}^{\infty} a_n G_n^{(1)} \frac{1}{s} J_{2n+2}(sl), \qquad G_n^{(1)}=\sqrt{\pi}(-1)^n \frac{\Gamma(2n+2+\frac{1}{2})}{(2n+1)!}, \tag{45}$$

$$\bar{f}_2(s)=\sum_{n=0}^{\infty} b_n G_n^{(2)} \frac{1}{s} J_{2n+1}(sl), \qquad G_n^{(2)}=\sqrt{\pi}(-1)^n \frac{\Gamma(2n+1+\frac{1}{2})}{(2n)!}, \tag{46}$$

where $\Gamma(x)$ and $J_n(x)$ are the Gamma and Bessel functions, respectively.

Substituting equations (45)–(46) into equations (37)–(40), it can be shown that equations (39)–(40) are automatically satisfied. After integration with respect to x in $[0, x]$, equations (37)–(38) reduce to

$$\begin{aligned} \frac{2}{\pi}\sum_{n=0}^{\infty}\int_0^{\infty} \frac{1}{s^2}[d_1(s)a_n G_n^{(1)} J_{2n+2}(sl) \\ +d_2(s)b_n G_n^{(2)} J_{2n+1}(sl)]\sin(sx)\mathrm{d}s=-\sigma_0 x, \quad 0\leqslant x\leqslant l, \end{aligned} \tag{47}$$

$$\begin{aligned} \sum_{n=0}^{\infty}\int_0^{\infty} \frac{1}{s^2}[d_3(s)a_n G_n^{(1)} J_{2n+2}(sl)+d_4(s)b_n G_n^{(2)} J_{2n+1}(sl)] \\ \times[\cos(sx)-1]\mathrm{d}s=0, \quad 0\leqslant x\leqslant l. \end{aligned} \tag{48}$$

From the relationships [22].

$$\int_0^{\infty} \frac{1}{s} J_n(sa)\sin(bs)\mathrm{d}s=\begin{cases} \dfrac{\sin[nsin^{-1}(b/a)]}{n}, & a>b, \\ \dfrac{a^n sin(n\pi/2)}{n[b+\sqrt{b^2-a^2}]^n}, & b>a, \end{cases} \tag{49}$$

$$\int_0^{\infty} \frac{1}{s} J_n(sa)\cos(bs)\mathrm{d}s=\begin{cases} \dfrac{\cos[nsin^{-1}(b/a)]}{n}, & a>b, \\ \dfrac{a^n cos(n\pi/2)}{n[b+\sqrt{b^2-a^2}]^n}, & b>a, \end{cases} \tag{50}$$

the semi-infinite integral in equations (47)–(48) can be modified as:

$$\begin{aligned} \int_0^{\infty} \frac{d_1(s)}{s^2} J_{2n+2}(sl)\sin(sx)\mathrm{d}s=\frac{\delta_1}{2n+2}\sin\left[(2n+2)\sin^{-1}\left(\frac{x}{l}\right)\right] \\ +\int_0^{\infty}\frac{1}{s}\left[\frac{d_1(s)}{s}-\delta_1\right] J_{2n+2}(sl)\sin(sx)\mathrm{d}s, \end{aligned} \tag{51}$$

$$\begin{aligned} \int_0^{\infty} \frac{d_2(s)}{s^2} J_{2n+1}(sl)\sin(sx)\mathrm{d}s=\frac{\delta_2}{2n+1}\sin\left[(2n+1)\sin^{-1}\left(\frac{x}{l}\right)\right] \\ +\int_0^{\infty}\frac{1}{s}[\frac{d_2(s)}{s}-\delta_2] J_{2n+1}(sl)\sin(sx)\mathrm{d}s, \end{aligned} \tag{52}$$

$$\int_0^\infty \frac{d_3(s)}{s^2} J_{2n+2}(sl)\cos(sx)\mathrm{d}s = \frac{\delta_2}{2n+2}\cos\left[(2n+2)\sin^{-1}\left(\frac{x}{l}\right)\right] + \int_0^\infty \frac{1}{s}[\frac{d_3(s)}{s} - \delta_2]J_{2n+2}(sl)\cos(sx)\mathrm{d}s, \tag{53}$$

$$\int_0^\infty \frac{d_4(s)}{s^2} J_{2n+1}(sl)\cos(sx)\mathrm{d}s = \frac{\delta_1}{2n+1}\cos\left[(2n+1)\sin^{-1}\left(\frac{x}{l}\right)\right] + \int_0^\infty \frac{1}{s}[\frac{d_4(s)}{s} - \delta_1]J_{2n+1}(sl)\cos(sx)\mathrm{d}s, \tag{54}$$

where

$$\lim_{s\to\infty} d_1(s)/s = \delta_1, \quad \lim_{s\to\infty} d_2(s)/s = \delta_2, \quad \lim_{s\to\infty} d_3(s)/s = \delta_2, \quad \lim_{s\to\infty} d_4(s)/s = \delta_1,$$

$$\delta_1 = \frac{\mu^{(2)}\mu^{(3)}[(-1+k^{(3)})\mu^{(2)} + \mu^{(3)} - \mu^{(3)}k^{(2)}]}{(\mu^{(2)} + \mu^{(3)}k^{(2)})(\mu^{(3)} + \mu^{(2)}k^{(3)})},$$

$$\delta_2 = -\frac{\mu^{(2)}\mu^{(3)}(\mu^{(2)} + k^{(3)}\mu^{(2)} + \mu^{(3)} + \mu^{(3)}k^{(2)})}{(\mu^{(2)} + \mu^{(3)}k^{(2)})(\mu^{(3)} + \mu^{(2)}k^{(3)})}.$$

$\delta_1 = \dfrac{\mu(k^{(3)} - k^{(2)})}{(1+k^{(2)})(1+k^{(3)})}$ and $\delta_2 = -\dfrac{\mu(2+k^{(2)}+k^{(3)})}{(1+k^{(2)})(1+k^{(3)})}$ for $\mu = \mu^{(3)}$ and $\beta = \dfrac{1}{h_2}ln(\dfrac{\mu^{(1)}}{\mu^{(3)}})$.

These constants can be obtained by using Mathematica (R). When $\mu = \mu^{(3)}$ and $\beta = \frac{1}{h_2}ln(\mu^{(1)}/\mu^{(3)})$, we have the same case as in [10]. The semi-infinite integral in equations (47) and (48) can be evaluated directly. Equations (47)and (48) can now be solved for the coefficients a_n and b_n by the Schmidt method [13,14]. For briefly, equations (47) and (48) can be rewritten as

$$\sum_{n=0}^{\infty} a_n E_n^*(x) + \sum_{n=0}^{\infty} b_n F_n^*(x) = U_0(x), \quad 0 \leqslant x \leqslant l, \tag{55}$$

$$\sum_{n=0}^{\infty} a_n G_n^*(x) + \sum_{n=0}^{\infty} b_n H_n^*(x) = 0, \quad 0 \leqslant x \leqslant l, \tag{56}$$

where $E_n^*(x)$, $F_n^*(x)$, $G_n^*(x)$ and $H_n^*(x)$ and $U_0(x)$ are known functions. The coefficients a_n and b_n are unknown.

From equation (56), it can be obtained:

$$\sum_{n=0}^{\infty} b_n H_n^*(x) = -\sum_{n=0}^{\infty} a_n G_n^*(x). \tag{57}$$

It can now be solved for the coefficients b_n by the Schmidt method [13–16]. Here the form $-\sum_{n=0}^{\infty} a_n G_n^*(x)$ can be considered as a known function temporarily. A set of functions $P_n(x)$, which satisfy the orthogonality condition

$$\int_0^l P_m(x) P_n(x) \mathrm{d}x = N_n \delta_{mn}, \quad N_n = \int_0^l P_n^2(x) \mathrm{d}x \tag{58}$$

can be constructed from the function, $H_n^*(x)$, such that

$$P_n(x) = \sum_{i=0}^{n} \frac{M_{in}}{M_{nn}} H_i^*(x), \tag{59}$$

where M_{ij} is the cofactor of the element d_{ij} of D_n, which is defined as

$$D_n = \begin{bmatrix} d_{00}, d_{01}, d_{02}, \ldots, d_{0n} \\ d_{10}, d_{11}, d_{12}, \ldots, d_{1n} \\ d_{20}, d_{21}, d_{22}, \ldots, d_{2n} \\ \cdots\cdots\cdots\cdots \\ \cdots\cdots\cdots\cdots \\ \cdots\cdots\cdots\cdots \\ d_{n0}, d_{n1}, d_{n2}, \ldots, d_{nn} \end{bmatrix}, \qquad d_{ij} = \int_0^l H_i^*(x) H_j^*(x) \mathrm{d}x. \tag{60}$$

Using equations (57)–(60), it can be obtained that

$$b_n = \sum_{j=n}^{\infty} q_j \frac{M_{nj}}{M_{jj}} \quad \text{with} \quad q_j = -\sum_{i=0}^{\infty} a_i \frac{1}{N_j} \int_0^l G_i^*(x) P_j(x) \mathrm{d}x. \tag{61}$$

Hence, it can be rewritten

$$b_n = \sum_{i=0}^{\infty} a_i K_{in}^*, \qquad K_{in}^* = -\sum_{j=n}^{\infty} \frac{M_{nj}}{N_j M_{jj}} \int_0^l G_i^*(x) P_j(x) \mathrm{d}x. \tag{62}$$

Substituting equation (62) into equation (55), it can be obtained

$$\sum_{n=0}^{\infty} a_n Y_n^*(x) = U_0(x), \qquad Y_n^*(x) = E_n^*(x) + \sum_{i=0}^{\infty} K_{ni}^* F_i^*(x). \tag{63}$$

So it can now be solved for the coefficients a_n by the Schmidt method again as mentioned above. With the aid of equation (62), the coefficients b_n can be obtained.

5. Stress Intensity Factors

The coefficients a_n and b_n are known, so that the entire stress field can be obtained. However, in fracture mechanics, it is important to determine stresses $\sigma_y^{(2)}$ and $\tau_{xy}^{(2)}$ in the vicinity of the crack tips. In the case of the present study, $\sigma_y^{(2)}$ and $\tau_{xy}^{(2)}$ along the crack line can be expressed as:

$$\sigma_y^{(2)}(x,0)=\frac{2}{\pi}\sum_{n=0}^{\infty}\int_0^{\infty}\frac{1}{s}[d_1(s)a_nG_n^{(1)}J_{2n+2}(sl)+d_2(s)b_nG_n^{(2)}J_{2n+1}(sl)]\cos(sx)\mathrm{d}s,$$
$$=\frac{2}{\pi}\sum_{n=0}^{\infty}\int_0^{\infty}\left\{\left[(\frac{d_1(s)}{s}-\delta_1)+\delta_1\right]a_nG_n^{(1)}J_{2n+2}(sl)\right.$$
$$\left.+\left[\left(\frac{d_2(s)}{s}-\delta_2\right)+\delta_2\right]b_nG_n^{(2)}J_{2n+1}(sl)\right\}\cos(sx)\mathrm{d}s, \tag{64}$$

$$\tau_{xy}^{(2)}(x,0)=\frac{2}{\pi}\sum_{n=0}^{\infty}\int_0^{\infty}\frac{1}{s}[d_3(s)a_nG_n^{(1)}J_{2n+2}(sl)+d_4(s)b_nG_n^{(2)}J_{2n+1}(sl)]\sin(sx)\mathrm{d}s,$$
$$=\frac{2}{\pi}\sum_{n=0}^{\infty}\int_0^{\infty}\left\{\left[(\frac{d_3(s)}{s}-\delta_2)+\delta_2\right]a_nG_n^{(1)}J_{2n+2}(sl)\right.$$
$$\left.+\left[\left(\frac{d_4(s)}{s}-\delta_1\right)+\delta_1\right]b_nG_n^{(2)}J_{2n+1}(sl)\right\}\sin(sx)ds. \tag{65}$$

An examination of equations (64) and (65) shows that, the singular parts of the stress fields can be obtained from the relationships as follows [22]:

$$\int_0^{\infty}J_n(sa)\cos(bs)\mathrm{d}s=\begin{cases}\dfrac{\cos[nsin^{-1}(b/a)]}{\sqrt{a^2-b^2}}, & a>b,\\ -\dfrac{a^n sin(n\pi/2)}{\sqrt{b^2-a^2}[b+\sqrt{b^2-a^2}]^n}, & b>a,\end{cases}$$

$$\int_0^{\infty}J_n(sa)\sin(bs)\mathrm{d}s=\begin{cases}\dfrac{\sin[nsin^{-1}(b/a)]}{\sqrt{a^2-b^2}}, & a>b,\\ \dfrac{a^n cos(n\pi/2)}{\sqrt{b^2-a^2}[b+\sqrt{b^2-a^2}]^n}, & b>a.\end{cases}$$

The singular parts of the stress fields can be expressed, respectively, as follows ($l<x$):

$$\sigma=-\frac{2\delta_2}{\pi}\sum_{n=0}^{\infty}b_nG_n^{(2)}H_n^{(1)}(x), \tag{66}$$

$$\tau=\frac{2\delta_2}{\pi}\sum_{n=0}^{\infty}a_nG_n^{(1)}H_n^{(2)}(x), \tag{67}$$

where $H_n^{(1)}(x)=\frac{(-1)^n l^{2n+1}}{\sqrt{x^2-l^2}[x+\sqrt{x^2-l^2}]^{2n+1}}$, $H_n^{(2)}(x)=\frac{(-1)^{n+1}l^{2n+2}}{\sqrt{x^2-l^2}[x+\sqrt{x^2-l^2}]^{2n+2}}$.

The stress intensity factors K_{I} and K_{II} can be given as follows

$$K_{\mathrm{I}}=\lim_{x\to l^+}\sqrt{2(x-l)}\cdot\sigma=-\frac{2\delta_2}{\sqrt{\pi l}}\sum_{n=0}^{\infty}b_n\frac{\Gamma(2n+1+\frac{1}{2})}{(2n)!}, \tag{68}$$

$$K_{\mathrm{II}} = \lim_{x\to l^+} \sqrt{2(x-l)}\cdot\tau = -\frac{2\delta_2}{\sqrt{\pi l}}\sum_{n=0}^{\infty} a_n \frac{\Gamma(2n+2+\frac{1}{2})}{(2n+1)!}. \tag{69}$$

After obtaining the stress intensity factors from equations (68) to (69), the strain energy release rate at the crack tip may be evaluated as follows

$$G(l) = \frac{\pi(k+1)}{8\mu}[K_{\mathrm{I}}^2(l) + K_{\mathrm{II}}^2(l)], \tag{70}$$

where $k=3-4\eta^{(2)}$ for plane strain, $k=(3-\eta^{(2)})/(1+\eta^{(2)})$for the plane stress.

6. Numerical Calculations and Discussion

To check the numerical accuracy of the Schmidt method, the values of $2\left[\sum_{n=0}^{9} a_n E_n^*(x) + \sum_{n=0}^{9} b_n F_n^*(x)\right]/(\pi\sigma_0)$ and $U_0(x)/\sigma_0$ are given in Table 1 for $\beta l=0.5$, $h_1/l=0.5$, $h_2/l=1.0$, $h_3/l=100.0$. In Table 2, the values of the coefficients a_n and b_n are given for $\beta l=0.5$, $h_1/l=0.5$, $h_2/l=1.0$, $h_3/l=100.0$.

As discussed in the works [13–16] and the above discussion, it can be found that the Schmidt method is performed satisfactorily if the first ten terms of infinite series in equations (55) and (56) are retained. The behavior of the sum of the series keeps steady with the increasing number of terms in equations (55) and (56). At $-l\leqslant x\leqslant l$, $y=0$, it can be obtained that $\sigma_y^{(2)}/\sigma_0$ is very close to negative unity. Hence, the solution of this paper can also be proved to satisfy the boundary conditions in equation (24). The homogeneous substrate, material '3', may be stiffer or softer with respect to homogeneous layer of ceramics, material '1'. The normalized non-homogeneity constant βl is varied between –3 and 3, which covers most of the practical cases. For the case in which the material constants of the material layers are different,

Table 1. Values of $2\left[\sum_{n=0}^{9} a_n E_n^*(x) + \sum_{n=0}^{9} b_n F_n^*(x)\right]/(\pi\sigma_0)$ and $U_0(x)/\sigma_0$ for $\beta l = 0.5$, $h_1/l = 0.5$, $h_2/l = 1.0$, $h_3/l=100.0$

	$2\left[\sum_{n=0}^{9} a_n E_n^*(x) + \sum_{n=0}^{9} b_n F_n^*(x)\right]/(\pi\sigma_0)$		
x	Real part	Imaginary part	$U_0(x)/\sigma_0$
0.1	−0.10001	0.0	−0.1
0.2	−0.20011	0.0	−0.2
0.3	−0.30006	0.0	−0.3
0.4	−0.40002	0.0	−0.4
0.5	−0.50012	0.0	−0.5
0.6	−0.60025	0.0	−0.6
0.7	−0.70012	0.0	−0.7
0.8	−0.80023	0.0	−0.8
0.9	−0.90018	0.0	−0.9

Table 2. Values of a_n and b_n for $\beta l = 0.5$, $h_1/l = 0.5$, $h_2/l = 1.0$, $h_3/l = 100.0$

	$2a_n/(\pi\sigma_0)$		$2b_n/(\pi\sigma_0)$	
n	Real part	Imaginary part	Real part	Imaginary part
0	0.265475D-03	0.0	−0.132231D-01	0.0
1	−0.469872D-04	0.0	−0.130567D-03	0.0
2	0.145972D-05	0.0	−0.516438D-04	0.0
3	−0.675762D-06	0.0	−0.106555D-04	0.0
4	0.822353D-07	0.0	−0.413480D-05	0.0
5	−0.158663D-07	0.0	−0.160736D-05	0.0
6	0.567221D-08	0.0	−0.720552D-07	0.0
7	−0.255342D-08	0.0	−0.520275D-08	0.0
8	0.103451D-08	0.0	−0.102215D-08	0.0
9	0.554138D-09	0.0	−0.564321D-09	0.0

the material constants of the ceramic layer are assumed as $\mu^{(1)} = 15.0(\times 10^9\mathrm{N/m^2})$ and $\eta^{(1)} = 0.2$, respectively. The material constants of the substrate layer are assumed as$\mu^{(3)} = 77.8(\times 10^9\mathrm{N/m^2})$ and $\eta^{(3)} = 0.33$, respectively. The material constants of the functionally graded materials are assumed as $\mu^{(2)} = 45.0e^{\beta y}(\times 10^9\mathrm{N/m^2})$ and $\eta^{(2)} = 0.28$, respectively. The dimensionless stress intensity factors $K/\sigma\sqrt{l}$ and the normalized strain energy release rate are calculated numerically. The results of this paper are shown in Figures 2–10. From the results, the following observations are very significant:

(i) It can be seen that the results of this paper is the same as ones in Ref. 10 when $\mu = \mu^{(3)}$ and $\beta = \frac{1}{h_2}\ln(\mu^{(1)}/\mu^{(3)})$ as shown in Figure 2 and Table 3. It is also proved that the Schmidt method is performed satisfactorily. However, in Ref. 10, the unknown variables of dual integral equations are the dislocation density functions, and the case of $\mu \neq \mu^{(3)}$ or $\beta \neq \frac{1}{h_2}\ln(\mu^{(1)}/\mu^{(3)})$ was not examined.

(ii) As the results given in Ref. 10, the stress intensity factors $K_{\mathrm{II}}/\sigma_0\sqrt{l}$ of this paper is not equal to zero for $\beta l = 0$. This phenomenon is cased by the thickness of the layer. This is quite different from ordinary cracks in homogeneous materials.

Table 3. Verification of the model ($h_1/l = 0.5, h_2/l = 1.0, h_3/l = 100.0$)

βl	$K_{\mathrm{I}}^*(l)/(\sigma_0\sqrt{l})$	$K_{\mathrm{I}}(l)/(\sigma_0\sqrt{l})$	$K_{\mathrm{II}}^*(l)/(\sigma_0\sqrt{l})$	$K_{\mathrm{II}}(l)/(\sigma_0\sqrt{l})$
−3.0	2.24	2.232	−0.58	−0.592
−2.5	2.03	2.029	−0.47	−0.479
−2.0	1.85	1.841	−0.38	−0.375
−1.5	1.67	1.667	−0.29	−0.284
−1.0	1.52	1.515	−0.21	−0.202
−0.5	1.39	1.383	−0.14	−0.133

Where $K_{\mathrm{I}}^*(l)/(\sigma_0\sqrt{l})$ and $K_{\mathrm{II}}^*(l)/(\sigma_0\sqrt{l})$ are Shbeeb's results [10]. $K_{\mathrm{I}}(l)/(\sigma_0\sqrt{l})$ and $K_{\mathrm{II}}(l)/(\sigma_0\sqrt{l})$ are this paper's results.

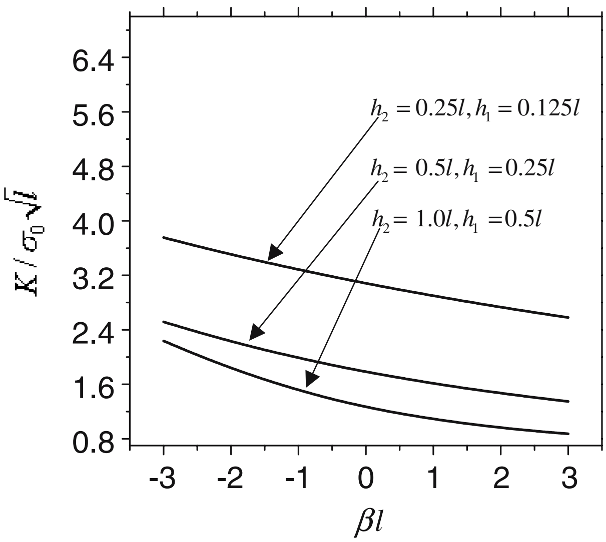

Figure 2. Influence of h_1/l and h_2/l on the normalized Mode-I SIF for $h_3/l = 100.0$ under a uniform normal stress loading when $\mu = \mu^{(3)}$ and $\beta = \frac{1}{h_2}\ln\left(\frac{\mu^{(1)}}{\mu^{(3)}}\right)$.

However, it can be obtained that the stress intensity factor $K_{\mathrm{II}}/\sigma_0\sqrt{l}$ tends to zero with the increase in the thickness of the medium layers for $\beta l = 0$ as shown in Figure 2.

(iii) When the material properties are not continuous along the crack line, an approximate solution of the interface crack problem is given under the assumption that the effect of the crack surface interference very near the crack tips is negligible. It can be obtained that the stress singularities of the present paper are the same as ones of the ordinary crack in homogeneous materials when the material parameters don't continue through the crack line. During the solving process for this case, the mathematical difficulties would not be met, i.e. the oscillatory stress singularity and the overlapping of the crack surfaces do not appeared near the interface crack tips, while much problems have to be considered when the material properties of the material layers are different.

(iv) The stress intensity factor $K_{\mathrm{I}}/\sigma\sqrt{l}$ decreases with the increase in the normalized non-homogeneity constant βl as shown in Figures 2 and 4. The shear stress intensity factor $K_{\mathrm{II}}/\sigma\sqrt{l}$ increases with the increase in the normalized non-homogeneity constant βl as shown in Figures. 3 and 5. A similar tendency was obtained in Ref. 10. However, the absolute values of the stress intensity factors for the case $\mu \neq \mu^{(3)}$ and $\beta \neq \frac{1}{h_2}\ln(\mu^{(1)}/\mu^{(3)})$ are larger than the ones for the case $\mu = \mu^{(3)}$ and $\beta = \frac{1}{h_2}\ln(\mu^{(1)}/\mu^{(3)})$ as shown from Figures 2–5.

(v) When $\mu \neq \mu^{(3)}$ and $\beta \neq \frac{1}{h_2}\ln(\mu^{(1)}/\mu^{(3)})$, the stress intensity factor $K_{\mathrm{I}}/\sigma\sqrt{l}$ tends to decrease with the increase in the thickness of the non-homogeneous layer, until reaching a minimum at $h_2/l \approx 0.8$, then it increases in magnitude as shown in Figure 6. However, the shear stress intensity factor $K_{\mathrm{II}}/\sigma\sqrt{l}$ tends to increase with the increase in the thickness of the non-homogeneous layer until reaching a peak, then it decreases in magnitude as shown in Figure 6. Hence, the stress field can reach a minimum value by changing the thickness of the non-homogeneity layer. This is quite

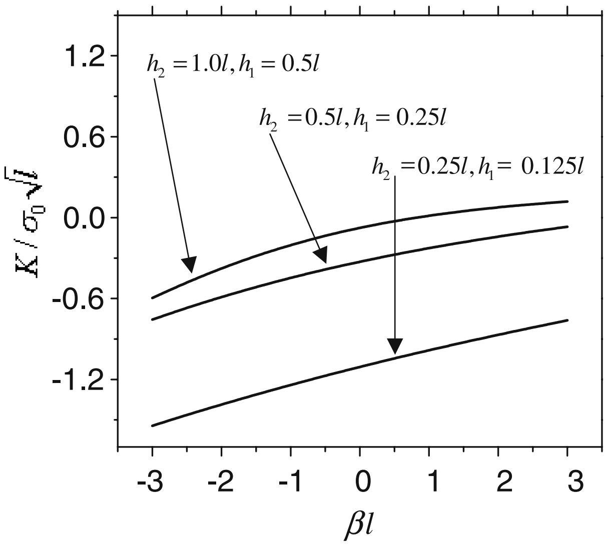

Figure 3. Influence of $h_1/l$and h_2/l on the normalized Mode-II SIF for $h_3/l=100.0$ under a uniform normal stress loading when $\mu=\mu^{(3)}$ and $\beta=\frac{1}{h_2}\ln\left(\frac{\mu^{(1)}}{\mu^{(3)}}\right)$.

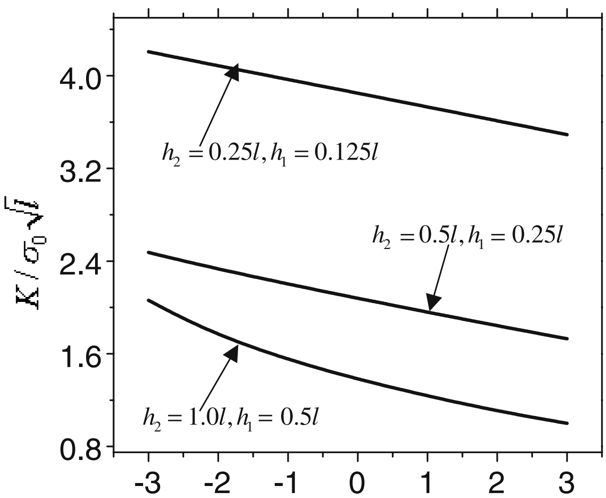

Figure 4. Influence of h_1/l and h_2/l on the normalized Mode-I SIF for $h_3/l=100.0$ under a uniform normal stress loading when $\mu\neq\mu^{(3)}$ and $\beta\neq\frac{1}{h_2}\ln\left(\frac{\mu^{(1)}}{\mu^{(3)}}\right)$.

different from the results as shown in Figure 6. For $\mu=\mu^{(3)}$ and $\beta=\frac{1}{h_2}ln(\mu^{(1)}/\mu^{(3)})$, the stress intensity factor $K_{\mathrm{I}}/\sigma\sqrt{l}$ tends to increase with the increase in the thickness of the non-homogeneous layer. The shear stress intensity factor $K_{\mathrm{II}}/\sigma\sqrt{l}$ tends to decrease with the increase in the thickness of the non-homogeneous layer as shown in Figure 7.

(vi) As shown in Figure 8, the stress intensity factor $K_{\mathrm{I}}/\sigma\sqrt{l}$ tends to decrease with the increase in the thickness of the ceramic layer. However, the shear stress intensity factor $K_{\mathrm{II}}/\sigma\sqrt{l}$ tends to increase with the increase in the thickness. This phenomenon is consistent with the crack in homogeneous materials.

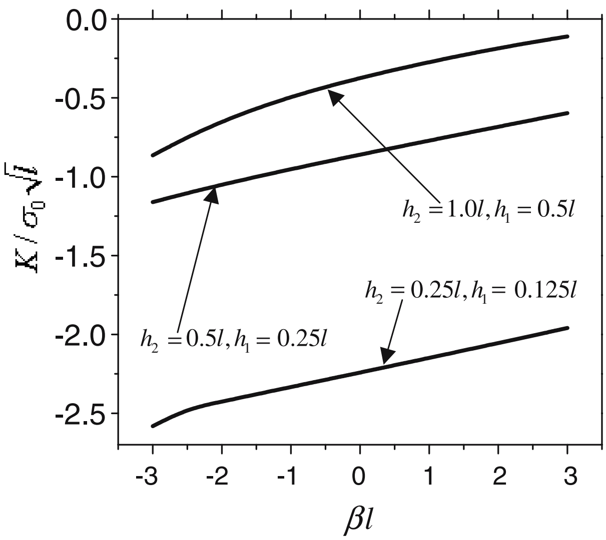

Figure 5. Influence of h_1/l and h_2/l on the normalized Mode-II SIF for $h_3/l = 100.0$ under a uniform normal stress loading when $\mu \neq \mu^{(3)}$ and $\beta \neq \frac{1}{h_2}\ln\left(\frac{\mu^{(1)}}{\mu^{(3)}}\right)$.

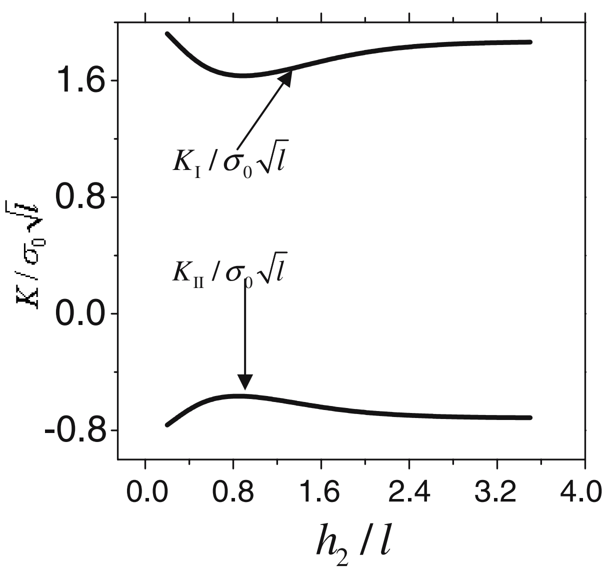

Figure 6. Influence of h_2/l on the normalized Mode-I and Mode-II SIF for $h_1/l = 1.0$, $h_3/l = 10.0$ and $\beta l = -2.0$ under a uniform normal stress loading when $\mu \neq \mu^{(3)}$ and $\beta \neq \frac{1}{h_2}\ln\left(\frac{\mu^{(1)}}{\mu^{(3)}}\right)$.

(vii) Figures 9 and 10 show the effect of the normalized non-homogeneity constant βl on the normalized strain energy release rate G/G_0 for uniform normal tractions $\sigma_y^{(2)}(x,0) = -\sigma_0$, $\sigma_{xy}^{(2)}(x,0) = 0$, where

$$G_0 = \frac{\pi(k+1)}{8\mu}\sigma_0^2 l \tag{71}$$

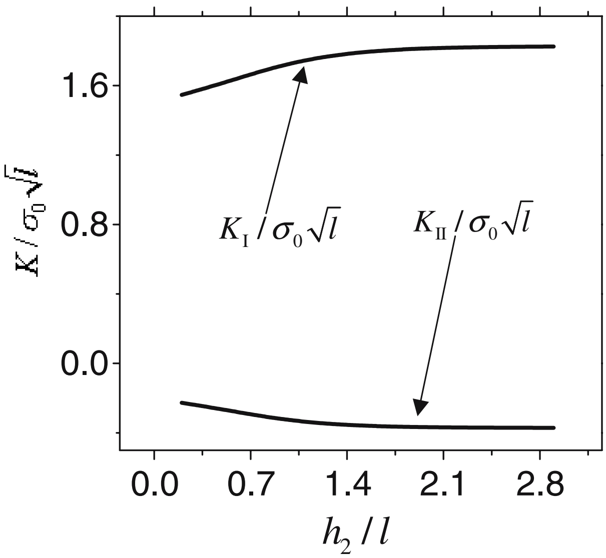

Figure 7. Influence of h_2/l on the normalized Mode-I and Mode-II SIF for $h_1/l = 1.0$, $h_3/l = 100.0$ and $\beta l = -2.0$ under a uniform normal stress loading when $\mu = \mu^{(3)}$ and $\beta = \frac{1}{h_2}\ln\left(\frac{\mu^{(1)}}{\mu^{(3)}}\right)$.

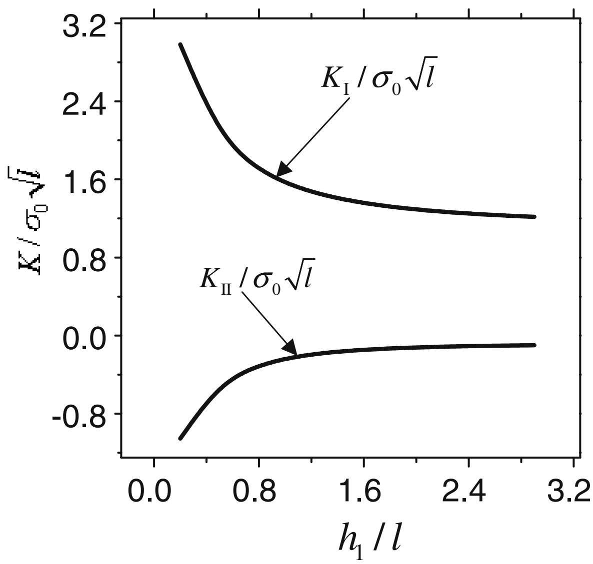

Figure 8. Influence of h_1/l on the normalized Mode-I and Mode-II SIF for $h_2/l = 0.25$, $h_3/l = 100.0$ and $\beta l = -2.0$ under a uniform normal stress loading when $\mu = \mu^{(3)}$ and $\beta = \frac{1}{h_2}\ln\left(\frac{\mu^{(1)}}{\mu^{(3)}}\right)$.

is the corresponding value for a homogeneous infinite medium with elastic constants μ and k. It can be noticed that the normalized strain energy release rate is significantly reduced by a small additional thickness of the functional graded material layer or the ceramics materials. The normalized strain energy release rate G/G_0 decreases with the increase in the normalized non-homogeneity constantβl as shown in Figures 9 and 10. These conclusions are the same as ones in Ref. 10. However, the normal-

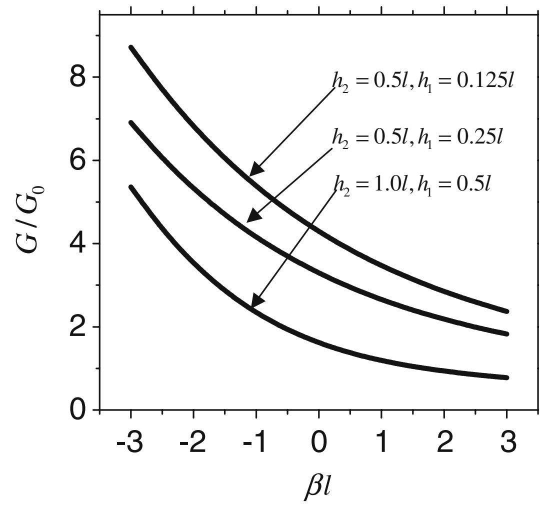

Figure 9. Influence of h_1/l and h_2/l on the normalized strain energy release rate for $h_3/l = 100.0$ under a uniform normal stress loading when $\mu = \mu^{(3)}$ and $\beta = \frac{1}{h_2}\ln\left(\frac{\mu^{(1)}}{\mu^{(3)}}\right)$.

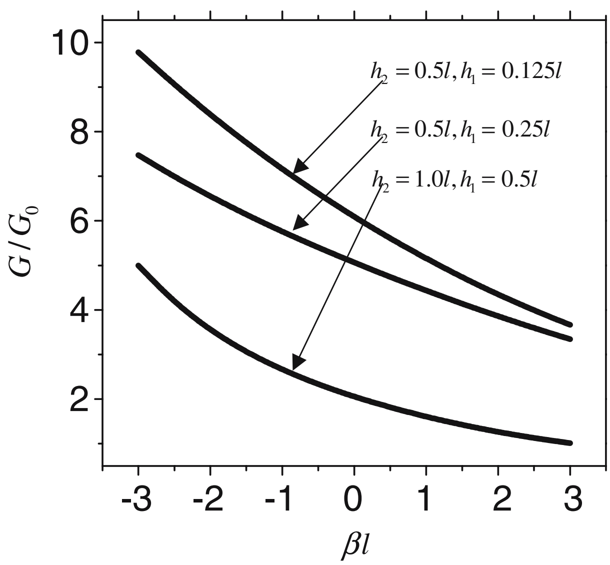

Figure 10. Influence of h_1/l and h_2/l on the normalized strain energy release rate for $h_3/l = 100.0$ under a uniform normal stress loading when $\mu \neq \mu^{(3)}$ and $\beta \neq \frac{1}{h_2}\ln\left(\frac{\mu^{(1)}}{\mu^{(3)}}\right)$.

ized strain energy release rates for the case $\mu \neq \mu^{(3)}$ and $\beta \neq \frac{1}{h_2}\ln(\mu^{(1)}/\mu^{(3)})$ are larger than the ones for the case $\mu = \mu^{(3)}$ and $\beta = \frac{1}{h_2}\ln(\mu^{(1)}/\mu^{(3)})$.

(viii) It can be concluded that the stress intensity factors can be reduced by several methods: stiffer coating application, thicker functional graded material layer, and additional layer of homogeneous ceramics. The most optimum combination depends on the stiffness ratio of the ceramics with respect to the substrate.

Acknowledgements

The authors are grateful for the financial support by the Natural Science Foundation with Excellent Yong Investigators of Hei Long Jiang Province (JC04–08), the Natural Science Foundation of Hei Long Jiang Province (A0301) and the National Natural Science Foundation of China (10572043, 10572155).

Appendix A

$$[X_1]=\mathrm{e}^{-s(h_1+h_2)}\begin{bmatrix} 2 & k^{(1)}-1+2s(h_1+h_2) \\ 2 & k^{(1)}-3+2s(h_1+h_2) \end{bmatrix},$$

$$[X_2]=\mathrm{e}^{s(h_1+h_2)}\begin{bmatrix} -2 & k^{(1)}-1-2s(h_1+h_2) \\ 2 & 3-k^{(1)}+2s(h_1+h_2), \end{bmatrix}$$

$$[X_3]=2s^2\mathrm{e}^{-sh_2}\begin{bmatrix} -1 & 1-sh_2 \\ -1 & 1-k^{(1)}-sh_2 \end{bmatrix}, \qquad [X_4]=2s^2\mathrm{e}^{sh_2}\begin{bmatrix} 1 & 1+sh_2 \\ -1 & k^{(1)}-1-sh_2 \end{bmatrix},$$

$$[X_5]=\begin{bmatrix} \mathrm{e}^{-\lambda_1 h_2} & \mathrm{e}^{-\lambda_2 h_2} \\ m_1(s)\mathrm{e}^{-\lambda_1 h_2} & m_2(s)\mathrm{e}^{-\lambda_2 h_2} \end{bmatrix}, \qquad [X_6]=\begin{bmatrix} \mathrm{e}^{-\lambda_3 h_2} & \mathrm{e}^{-\lambda_4 h_2} \\ m_3(s)\mathrm{e}^{-\lambda_3 h_2} & m_4(s)\mathrm{e}^{-\lambda_4 h_2} \end{bmatrix},$$

$$[X_7]=2\mu^{(1)}s^3\mathrm{e}^{-sh_2}\begin{bmatrix} 2 & k^{(1)}-1+2sh_2 \\ 2 & k^{(1)}-3+2sh_2 \end{bmatrix}, \quad [X_8]=2\mu^{(1)}s^3\mathrm{e}^{sh_2}\begin{bmatrix} -2 & k^{(1)}-1-2sh_2 \\ 2 & 3-k^{(1)}+2sh_2 \end{bmatrix},$$

$$[X_9]=\mu\mathrm{e}^{\beta h_2}\begin{bmatrix} \frac{[-(k^{(2)}+1)m_1(s)\lambda_1+s(3-k^{(2)})]\mathrm{e}^{-\lambda_1 h_2}}{k^{(2)}-1} & \frac{[-(k^{(2)}+1)m_2(s)\lambda_2+s(3-k^{(2)})]\mathrm{e}^{-\lambda_2 h_2}}{k^{(2)}-1} \\ [-\lambda_1-sm_1(s)]\mathrm{e}^{-\lambda_1 h_2} & [-\lambda_2-sm_2(s)]\mathrm{e}^{-\lambda_2 h_2} \end{bmatrix},$$

$$[X_{10}]=\mu\mathrm{e}^{\beta h_2}\begin{bmatrix} \frac{[-(k^{(2)}+1)m_3(s)\lambda_3+s(3-k^{(2)})]\mathrm{e}^{-\lambda_3 h_2}}{k^{(2)}-1} & \frac{[-(k^{(2)}+1)m_4(s)\lambda_4+s(3-k^{(2)})]\mathrm{e}^{-\lambda_4 h_2}}{k^{(2)}-1} \\ [-\lambda_3-sm_3(s)]\mathrm{e}^{-\lambda_3 h_2} & [-\lambda_4-sm_4(s)]\mathrm{e}^{-\lambda_4 h_2} \end{bmatrix},$$

$$[X_{11}]=\mathrm{e}^{sh_3}\begin{bmatrix} 2 & k^{(3)}-1-2sh_3 \\ 2 & k^{(3)}-3-2sh_3 \end{bmatrix}, \qquad [X_{12}]=\mathrm{e}^{-sh_3}\begin{bmatrix} -2 & k^{(3)}-1+2sh_3 \\ 2 & 3-k^{(3)}-2sh_3 \end{bmatrix},$$

$$[X_{13}]=2\mu^{(3)}s^3\begin{bmatrix} 2 & k^{(3)}-1 \\ 2 & k^{(3)}-3 \end{bmatrix}, \qquad [X_{14}]=2\mu^{(3)}s^3\begin{bmatrix} -2 & k^{(3)}-1 \\ 2 & 3-k^{(3)} \end{bmatrix},$$

$$[X_{15}]=\mu\begin{bmatrix} \frac{-(k^{(2)}+1)m_1(s)\lambda_1+s(3-k^{(2)})}{k^{(2)}-1} & \frac{-(k^{(2)}+1)m_2(s)\lambda_2+s(3-k^{(2)})}{k^{(2)}-1} \\ -\lambda_1-sm_1(s) & -\lambda_2-sm_2(s) \end{bmatrix},$$

$$[X_{16}]=\mu\begin{bmatrix}\dfrac{-(k^{(2)}+1)m_3(s)\lambda_3+s(3-k^{(2)})}{k^{(2)}-1} & \dfrac{-(k^{(2)}+1)m_4(s)\lambda_4+s(3-k^{(2)})}{k^{(2)}-1}\\ -\lambda_3-sm_3(s) & -\lambda_4-sm_4(s)\end{bmatrix},$$

$$[X_{17}]=\begin{bmatrix}1 & 1\\ m_1(s) & m_2(s)\end{bmatrix},\qquad [X_{18}]=\begin{bmatrix}1 & 1\\ m_3(s) & m_4(s)\end{bmatrix},\qquad [X_{19}]=2s^2\begin{bmatrix}-1 & 1\\ -1 & 1-k^{(3)}\end{bmatrix},$$

$$[X_{20}]=2s^2\begin{bmatrix}1 & 1\\ -1 & k^{(3)}-1\end{bmatrix},\qquad [Y_1]=[X_3]-[X_4][X_2]^{-1}[X_1],$$

$$[Y_2]=[X_7]-[X_8][X_2]^{-1}[X_1],$$

$$[Y_3]=[Y_1]^{-1}[X_5]-[Y_2]^{-1}[X_9],\quad [Y_4]=[Y_2]^{-1}[X_{10}]-[Y_1]^{-1}[X_6],\quad [Y_5]=[Y_4]^{-1}[Y_3],$$

$$[Y_6]=-[X_{13}][X_{11}]^{-1}[X_{12}]+[X_{14}],\qquad [Y_7]=[X_{15}]+[X_{16}][Y_5],\quad [Y_8]=[Y_6]^{-1}[Y_7],$$

$$[Y_9]=[X_{17}]+[X_{18}][Y_5],\quad [Y_{10}]=-[X_{19}][X_{11}]^{-1}[X_{12}]+[X_{20}],[Y_{11}]=[Y_9]-[Y_{10}][Y_8],$$

$$[Y_{12}]=[X_{15}]+[X_{16}][Y_5],\qquad [Y_{13}]=[Y_{12}][Y_{11}]^{-1}=\begin{bmatrix}d_1(s) & d_2(s)\\ d_3(s) & d_4(s)\end{bmatrix}.$$

References

1. Koizumi, M., ‘The concept of FGM’. in: Holt, J.B. et al. (eds.), *Ceramic Transactions* Vol. 34, Functionally Graded Materials. American Ceramic Society, Ohio, pp. 3–10.
2. Lee, Y.D. and Erdogan, F., ‘Residual/thermal stress in FGM and laminated thermal barrier coating’, *Int. J. Fract.*, **69** (1994) 145–165.
3. Suresh, S. and Mortensen, A., ‘Functionally graded metals and metal-ceramic composites: part 2 thermomechanical behaviour’, *Int. Mater. Rev.* **29** (1977) 306–312.
4. Choi, H.J., ‘The problem for bonded half-planes containing a crack at an arbitrary angle to the graded interfacial zone’, *Int. J. Solids Struct.* **38** (2001) 6559–6588.
5. Delae, F. and Erdogan, F., ‘On the mechanical modeling of the interfacial region in bonded half-planes’, *ASME J. Appl. Mech* **55** (1988) 317–324.
6. Ozturk, M. and Erdogan, F., ‘Axisymmetric crack problem in bonded materials with a graded interfacial region’, *Int. J. Solids Strut*. **33** (1996) 193–219.
7. Chen, Y.F., ‘Interface crack in nonhomogeneous bonded materials of finite thickness’, Ph.D. Dissertation, Lehigh University (1990).
8. Jin, Z.H. and Batra, R.C., ‘Interface cracking between functionally graded coating and a substrate under antiplane shear’, *Int. J. Eng. Sci.* **34** (1996) 1705–1716.
9. Bao, G. and Cai, H., ‘Delamination cracking in functionally graded coating/metal substrate systems’, *ACTA Materialia* **45** (1997) 1055–1066.
10. Shbeeb, N.I. and Binienda, W.K., ‘Analysis of an interface crack for a functionally graded strip sandwiched between two homogeneous layers of finite thickness’, *Eng. Frac. Mech.* **64** (1999) 693–720.
11. Wang, B.L., Han, J.C. and Du, S.Y., ‘Crack problem for non-homogeneous composite materials subjected to dynamic loading’, *Int. J. Solids Struct*. **37** (2000) 1251–1274.
12. Erdogan, F. and Wu, H.B., ‘Crack problems in FGM layer under thermal stress’, *J. Thermal Stress* **19** (1996) 237–265.

13. Morse, P.M. and Feshbach, H., *Methods of Theoretical Physics*, Vol.1, McGraw-Hill, New York, 1958, p. 926.
14. Zhou, Z.G., Liang, J. and Wang, W., Two collinear permeable cracks in a piezoelectric layer bonded to two half spaces, *Meccanica* **38** (2003) 467–475.
15. Zhou, Z.G., Chen, J.Y. and Wang, B., 'Analysis of two collinear cracks in a piezoelectric layer bonded to two half spaces subjected to anti-plane shear', *Meccanica* **35** (2000) 443–456.
16. Zhou, Z.G., Sun, Y.G. and Wang, B., 'Investigation of the dynamic behavior of a Griffith crack in a piezoelectric material strip subjected to the harmonic elastic anti-plane shear waves by use of the non-local theory', *Meccanica* **39** (1) (2004) 63–76.
17. Itou, S., 'Stresses around an interface crack', *Eng. Fract. Mech*. **25** (1986) 415–420.
18. England, A.H., 'A crack between dissimilar media', *J. Appl. Mech*. **32** (1965) 400–402.
19. Erdogan, F. and Wu, B.H., Interface crack problems in layered orthotropic materials, *J. Mech. Phys. Solids'*, **41**(5) (1993) 889–917.
20. Zhang, X.S., 'A central crack at the interface between two different orthotropic media for the mode I and mode II', *Eng. Fract. Mech.* **33**(3) (1989) 327–333.
21. Zhang, X.S., 'A center crack at the interface between two different media for the opening mode', *Eng. Fract. Mech*. **24** (2) (1986) 177–185.
22. Gradshteyn, I.S. and Ryzhik, I.M., *Table of Integrals, Series and Products*, Academic Press, New York, 1980.
23. Erdelyi, A. (ed), *Tables of Integral Transforms*, Vol.1, McGraw-Hill, New York, (1954).